

Capture Gamma Rays from the Proton Bombardment of Be^9 †

W. F. HORNYAK AND T. COOR
Brookhaven National Laboratory, Upton, New York
 (Received July 28, 1953)

The gamma rays produced at the 0.993- and 1.085-Mev proton capture resonances in Be^9 were studied using a NaI scintillation spectrometer. Gamma rays of energies 0.41, 0.72, 1.02, 1.43, and 7.5 Mev, and energies 0.72, 1.43, 2.0–2.5, and 6.8₀ Mev were observed for the two levels, respectively. Absolute yields were determined, and the possible decay schemes are discussed.

1. INTRODUCTION

THE excitation function for proton capture radiation from Be^9 has been extensively studied,¹ with numerous resonances being evident. The radiative decay of the broad resonance observed at 998 ± 4 kev (7.48-Mev excitation in B^{10}) was found to proceed mostly by the direct transition to the ground state of B^{10} giving a 7.38 ± 0.07 -Mev^{2,3} gamma ray with a thick target (Be metal) yield of $17.8 \gamma/10^9 p$.⁴ The radiation from the narrow resonance at 1087 ± 2 kev (7.56-Mev excitation in B^{10}) was found to consist predominantly of 6.8- and 0.72-Mev gamma rays of approximately equal intensity, indicating the major mode of decay to be a cascade through the first excited state in B^{10} at 0.72 Mev.^{3,5} The thick target yield was observed to be $1.01 \gamma/10^9 p$.⁴

The object of this experiment is to investigate further the nature of the capture radiation from these two resonances.

2. APPARATUS

The Brookhaven electrostatic accelerator was used to supply protons for the bombardment of various Be targets mounted in a thin wall (0.015 in.) brass target holder. The gamma-ray detector was a NaI scintillation crystal, 4 cm in diameter and 3 cm in height, used in conjunction with an electronic single-channel pulse-height analyser. The source to detector distance was 2.0 cm, measured from the center of the $\frac{3}{8}$ -in. diameter collimated proton beam to the front flat face of the crystal, the cylindrical axis of the crystal being at 90° relative to the beam. Lead shielding was used to reduce the background, notably the x-rays from the several tantalum collimators used. This shielding was found necessary to reduce the electronic pile up of pulses and the resulting lowering of the resolution of the various lines observed in the scintillation pulse height spectrum.

† Research done at Brookhaven National Laboratory under contract with the U. S. Atomic Energy Commission.

¹ F. Ajzenberg and T. Lauritsen, *Revs. Modern Phys.* **24**, 231 (1952).

² R. L. Walker (private communication).

³ Fowler, Lauritsen, and Lauritsen, *Revs. Modern Phys.* **20**, 236 (1948).

⁴ W. A. Fowler and C. C. Lauritsen, *Phys. Rev.* **76**, 314 (1949).

⁵ Lauritsen, Fowler, Lauritsen, and Rasmussen, *Phys. Rev.* **73**, 636 (1948).

3. DETECTOR CALIBRATION

The differential pulse-height spectrum for various gamma rays observed with the NaI crystal used in this experiment is shown in Fig. 1. The sources consisted of the 1.28-Mev γ ray from Na^{22} , the 3.08-Mev γ ray from $\text{C}^{12}(d,p\gamma)$, and the 6.13-Mev γ ray from $\text{F}^{19}(p,\alpha\gamma)$ at the 340-kev resonance. Only the total conversion line and the Compton electron peak are detected for the lowest energy γ ray, the pair production being relatively small. For the higher-energy γ rays, the annihila-

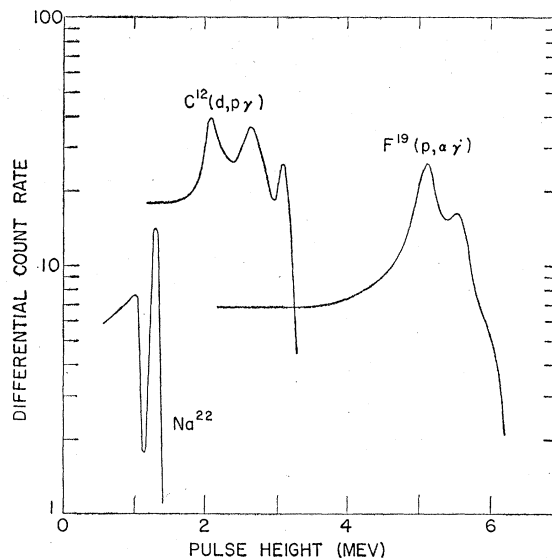


FIG. 1. The differential pulse-height spectrum for a NaI crystal (4 cm in diameter and 3 cm in height) irradiated by several γ -ray sources; Na^{22} —1.28 Mev, $\text{C}^{12}(d,p\gamma)$ —3.08 Mev, and $\text{F}^{19}(p,\alpha\gamma)$ —6.13 Mev.

tion quantum escape peaks are seen to gain in prominence as the incident gamma-ray energy is raised.

The counting rate observed at any of the line structures described above, with a unit strength source, will in general depend in a complicated way on the geometry and the various electro-magnetic cross sections, the division of the total effect into "solid angle" and "efficiency" being to a large extent arbitrary. For example, the attempt to define solid angle along conventional lines leads in general to efficiencies which are functions of source to detector distance as well as

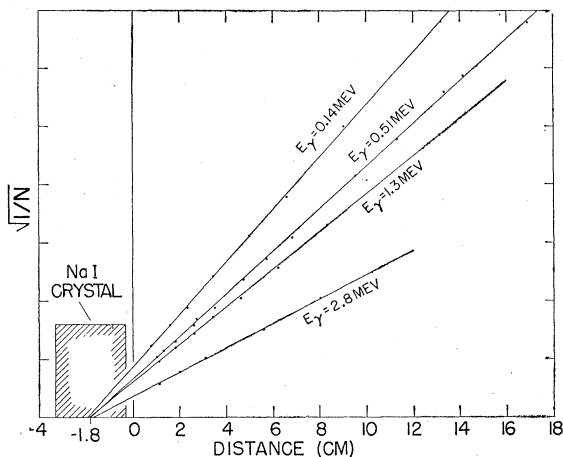


FIG. 2. The variation of $1/N^2$, where N is the counting rate at the total conversion line peak, with the source to detector distance for several γ -ray sources. The NaI crystal was mounted in a $\frac{3}{8}$ -in. thick Al can packed with MgO as a reflector.

of gamma-ray energy. It was found (refer to Fig. 2) that the count rate with the channel discriminator set to the total conversion line peak could be empirically fitted with an "inverse square law,"

$$N \propto (d+x)^{-2},$$

with x the distance from the source to the front face of the crystal and with d a constant relatively independent of gamma-ray energy. Thin sources under $\frac{1}{4}$ in. in diameter were used and located on the axis of symmetry of the crystal. This law was found to hold to ± 5 percent for $x \geq 1.0$ cm, $E_\gamma \geq 140$ kev, and with $d = 1.5$ cm. The entire variation of d with energy is within ± 0.1 cm. The area to be used with the inverse square law was arbitrarily taken as the cross-sectional area of the crystal used in this experiment, which was 4π cm². Thus, the "solid angle" for this particular crystal may be written as

$$\Omega = (x+1.5)^{-2} \text{ fraction of a sphere,} \quad (1)$$

with x in cm.

Coincidence γ - γ and β - γ counting with Na²²,⁶ Na²⁴, Co⁶⁰, and Au¹⁹⁸ were used to determine the efficiency from the area under the total conversion line, the effect of the electronic channel width being appropriately corrected for each time. The results are given in Fig. 3. An interesting check on the efficiency curve thus obtained was made using the single γ -ray emitting source Cs¹³⁷. The discriminator was set to count all pulses above tube noise (appropriate extrapolations to zero pulse height were made). The discriminator was then set to a narrow channel and the area under the total conversion line determined. After an experimental correction is made to the integral count rate, necessitated by the internal conversion x-ray in Cs¹³⁷, a

⁶ During the course of this work a K -capture branch in Na²² of 7.1 ± 2.0 percent was discovered.

comparison of this rate with the rate observed under the total conversion line gives the efficiency for the latter, since the efficiency for the former may be readily calculated. In this comparison it is also necessary to determine the appropriate d in the solid angle expression for the case of the integral pulse-height counting (this experiment was restricted to large source to detector distances).

The efficiency for counting all scintillation events is calculated from the total absorption coefficient, which for the Cs¹³⁷ γ ray (0.662 Mev) is 0.276 cm^{-1} .^{7,8} The calculation is simple when the variation of the solid angle over the crystal is kept small by using a large source to detector distance. The effect resulting from partial energy transfer to the scintillator by electrons or scattered γ rays escaping through the surface is negligible due to the high signal-to-noise ratio generally realized. A considerable simplification results from the fact that multiple processes in the interactions of the γ ray within the NaI crystal need not be considered since the phosphor decay time and amplifier response time are long compared to the time within which all such multiple interactions occur.

The resulting total conversion line efficiency for Cs¹³⁷ is also given in Fig. 3. The point on this curve at 6.1 Mev was obtained from the F¹⁹($p, \alpha \gamma$) reaction using a thick CaF₂ target and $E_p = 370$ kev. The yield was taken as $16.4 \gamma/10^9 p$, the average of the absolute γ -ray determination and the absolute α -particle deter-

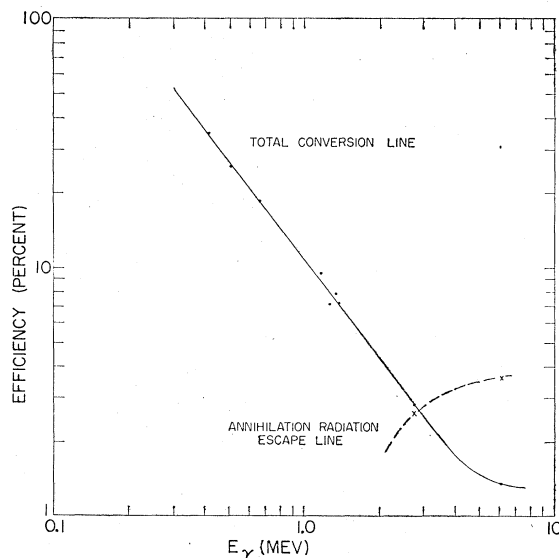


FIG. 3. The measured efficiency for a NaI crystal (4 cm in diameter and 3 cm in height) as determined by the area under the total conversion lines and the area under the two quantum annihilation radiation escape lines. The experimental errors on the points are ± 5 percent, except for the points at 6.1 Mev where the error is ± 15 percent.

⁷ G. R. White, National Bureau of Standards Report 1003, 1952 (unpublished).

⁸ C. M. Davisson and R. D. Evans, Revs. Modern Phys. **24**, 79 (1952).

mination obtained by previous experimenters.^{8,9} The part of the efficiency curve below 3.5 Mev can be fitted with the expression

$$\eta = 10.6E_\gamma^{-1.31} \text{ percent}, \quad (2)$$

with E_γ in Mev. The two points on the annihilation radiation escape peak curve of Fig. 3 were obtained using Na^{24} and $\text{F}^{19}(p,\alpha\gamma)$ sources.

4. RESULTS

The differential pulse-height spectrum of γ rays, having energies below 2 Mev, obtained with a thick Be metal target bombarded at 0.860 and 1.060 Mev, and a thin (4-kev) evaporated Be metal target bombarded at 1.085 Mev are shown in Fig. 4. The beam current was limited to less than $1 \mu\text{a}$ with the thin

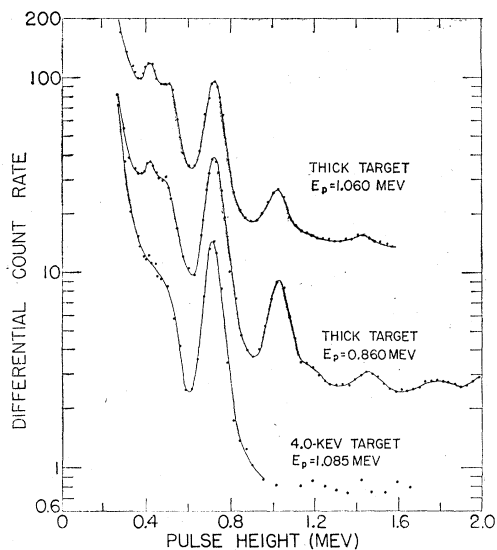


FIG. 4. The differential pulse-height spectrum for $\text{Be}^9(p,\gamma)$ γ rays below 2.0 Mev for several bombardment conditions.

target to prevent its deterioration. The energies of the prominent total conversion lines were determined by comparison with the lines produced by the 0.511- and 1.277-Mev radiations from Na^{22} . The resulting energies are 0.414 ± 0.01 , 0.716 ± 0.01 , 1.02 ± 0.01 , 1.43 ± 0.01 , and 1.78 ± 0.02 Mev. Only a continually rising background was observed below 0.4 Mev, with any possible structure being obscured by background not originating in the target reaction. The prominent edge at 0.51 Mev is due partly to the Compton line of the 0.72-Mev radiation and to annihilation radiation from the lead shield produced by energetic γ rays. This latter point was checked by varying the shield geometry. The interpretation of the anomaly at ~ 1.2 Mev is not clear.

The differential pulse-height spectrum for the energetic γ rays under identical bombardment conditions

⁸ Chao, Tollestrup, Fowler, and Lauritsen, Phys. Rev. **79**, 108 (1950).

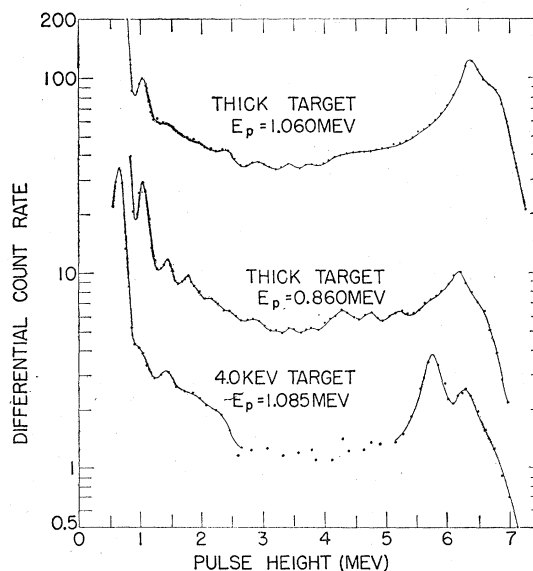


FIG. 5. The differential pulse-height spectrum for $\text{Be}^9(p,\gamma)$ γ rays for several bombardment conditions.

is shown in Fig. 5. In each case the strongest prominence near the high-energy end of the spectrum is interpreted as the two annihilation quanta escape peak, $E_\gamma - 1.02$ Mev, of the highest energy γ ray present (compare with Fig. 1). The γ -ray energies obtained for the thick target runs at $E_p = 0.860$ and 1.060 Mev are 7.1 and 7.4 Mev, respectively, and 6.89 ± 0.1 for the thin target run at $E_p = 1.085$ Mev. In addition, it is noted that the one-annihilation-quantum escape peak, $E_\gamma - 0.51$ Mev, is clearly resolved for the case of the thin-target run and is only barely evident for the thick-target runs because of the energy spread resulting from the reaction proceeding at all energies below the incident proton beam energy. Although the anomalies in

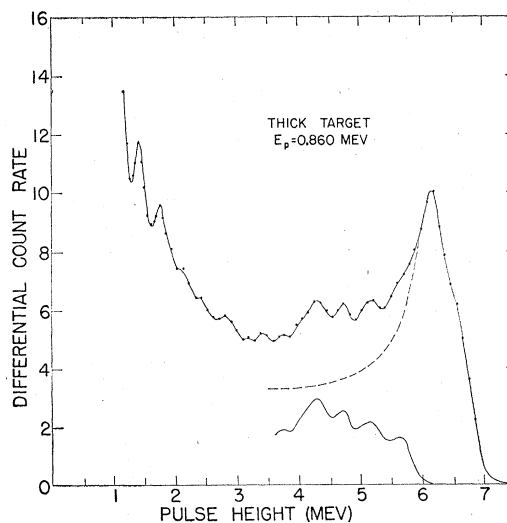


FIG. 6. The differential pulse-height spectrum for $\text{Be}^9(p,\gamma)$ γ rays, showing the resolving of the structure above 4 Mev.

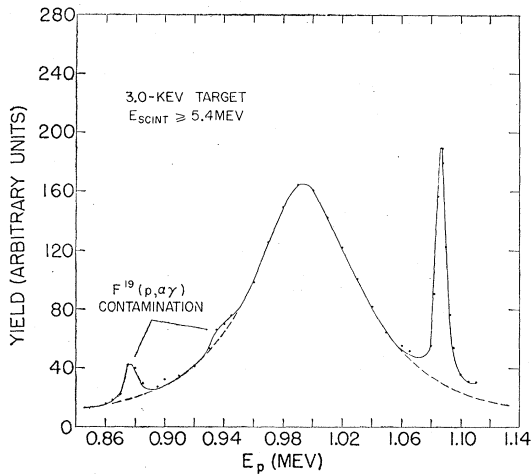


FIG. 7. The thin target $\text{Be}^9(p,\gamma)$ yield of energetic scintillation events. The fluorine contamination was introduced to establish the proton energy scale. The dashed curve represents a single-level dispersion formula fit of the experimental points.

the curves between scintillation energies of 2–4 Mev are reproducible, their interpretation is not clear except perhaps for the peak at 2.1₅ Mev which is probably a total conversion line. Figure 6 is a linear scale plot of the thick target data taken at $E_p=0.860$ Mev to emphasize the resolution of the structure above 4 Mev. The simplest interpretation of the four peaks at 4.2, 4.7, 5.1, and 5.6 Mev is that they are the two- and one-annihilation-quantum escape peaks of two γ rays of energy 5.2 and 6.1 Mev.

With the discriminator set to accept scintillation pulses greater than 5.3₅ Mev, the thin target (3-kev) yield curve of Fig. 7 was obtained. A small amount of fluorine contamination of the beryllium target was introduced to establish the voltage scale through the $\text{F}^{19}(p,\alpha\gamma)$ resonances at 874 and 935 keV. Resonance energies for the $\text{Be}^9(p,\gamma)$ reaction of 993 ± 2 and 1085 ± 2 were determined, correction for the target thickness

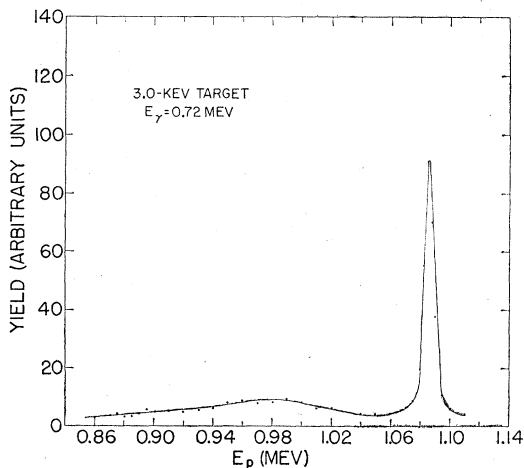


FIG. 8. The thin-target $\text{Be}^9(p,\gamma)$ yield of 0.72-Mev γ radiation.

having been made. It was found that the broad resonance could be fitted with a one-level dispersion formula (the dotted line extensions of the curve in Fig. 7). The total level width found was 88 ± 3 keV. No direct determination of the width of the narrow resonance was made although the value of 4 keV obtained by Fowler and Lauritsen⁴ was found to be consistent with the present results.

Figure 8 shows the thin-target (3-kev) excitation function obtained when the discriminator channel was set on the 0.72-Mev line. The corresponding thick Be metal target yield is given in Fig. 9. The background of higher energy γ rays falling in the channel has been corrected for, the correction never exceeding 15 percent. In all cases the thickness of the thin targets was determined by a comparison of the resonant thin-target yield of 0.72-Mev radiation with the corre-

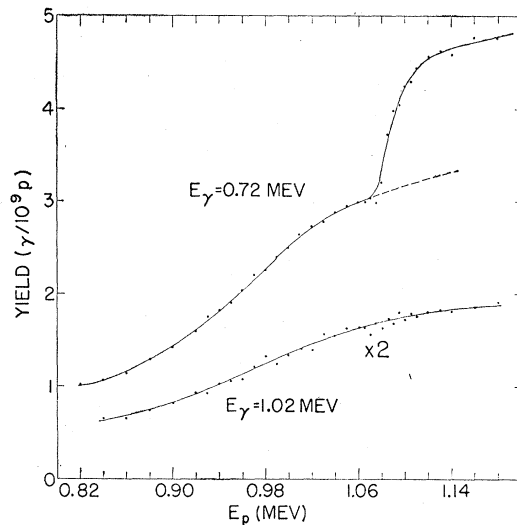


FIG. 9. The thick-target $\text{Be}^9(p,\gamma)$ yields of 0.72- and 1.02-Mev γ radiations.

sponding “step” in the thick-target yield. Also shown in Fig. 9 is the thick-target yield of 1.02-Mev radiation. In this case the aforementioned background correction varied from 20 to 48 percent. Note the absence of any prominent rise in the yield at the narrow resonance.

The absolute thick (Be metal) target yield of the γ radiation found in this experiment is given in Table I. In these determinations absolute counting rates for $E_\gamma < 3$ Mev were determined by measuring areas under the total conversion lines and using the appropriate NaI calibration of Fig. 3 and Eq. (1). In the case of the 5.2- and 6.2-Mev radiations the areas under the peaks ascribed to the two annihilation quantum escape lines were used. The estimate of the yield of 2.0–2.5 Mev radiation for the narrow resonance was made on the basis of a rough comparison with Na^{24} .

In each case of Table I the absolute count rate of the most energetic γ ray was determined by a comparison of the total area above a pulse height $0.92(E_{\gamma \text{ max}} - 1.02)$

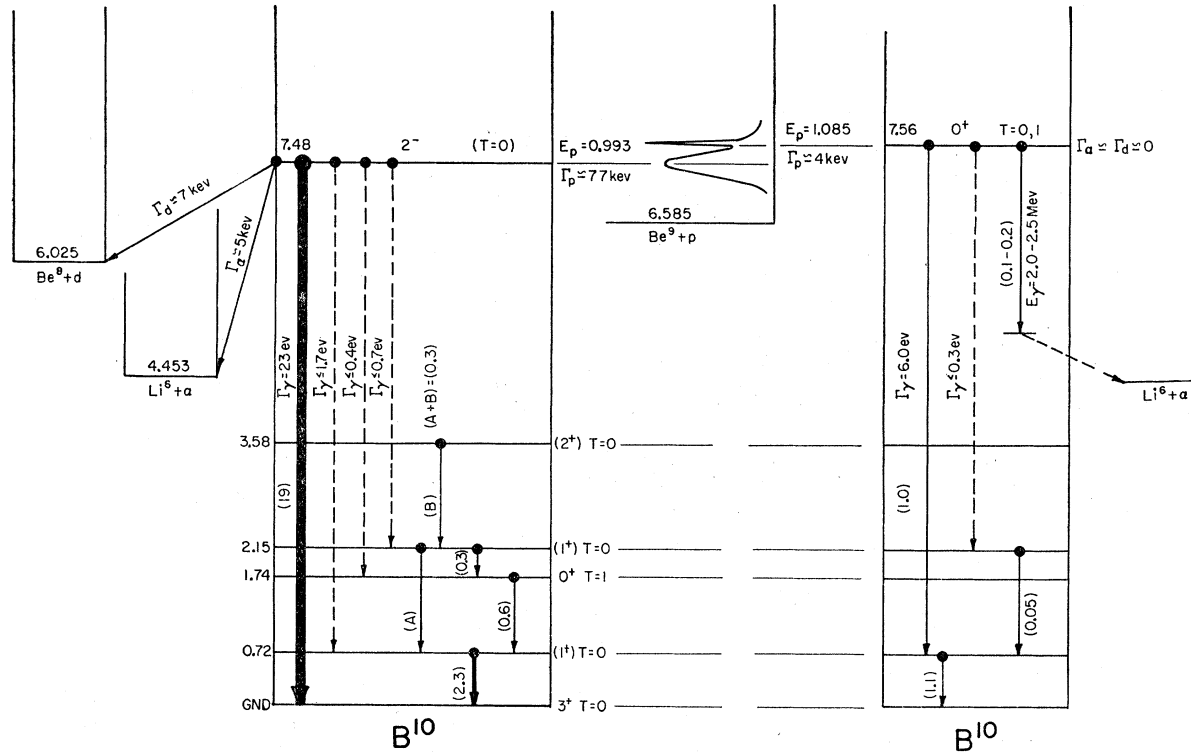


FIG. 10. The decay modes of the two prominent Be^9p resonances. All energy units are in Mev except where specifically otherwise noted. The quantities in parentheses labeling the γ -ray transitions are $\gamma/10^9p$. The sum of the transitions A and B is indicated, $A \gg B$. The other quantities in parentheses represent tentative spin and parity, or isotopic spin assignments. The dotted transitions are inferred and have not been experimentally observed.

Mev with the corresponding area for the $\text{F}^{19}(p,\alpha\gamma)$ radiation. Appropriate corrections for the variation of γ -ray cross sections with energy were made. The above procedure to a large extent avoids the problems arising from the use made of thick targets in some of the runs.

The yield of 0.72-Mev radiation originating from the narrow resonance was determined from the step in the thick target curve of Fig. 9. The yields of the other radiations from the narrow resonance were then determined from the absolute counting rates observed in Figs. 4 and 5, relative to the 0.72-Mev line. The yields of the 0.72- and 1.02-Mev radiations from the broad resonance were determined by fitting integrated dispersion formula yields to the thick-target curves of Fig. 9. The difference in absolute counting rates at 1.060 and 0.860 Mev for the other radiations relative to the corresponding difference for the 0.72- and 1.02-Mev lines was used to calculate the remaining absolute yields.

5. DISCUSSION OF RESULTS

The yield of the various γ radiations from the narrow resonance (refer to Table I, and Fig. 10) substantiate the results observed by previous investigators in that the principle mode of decay is through the first excited state in B^{10} at 0.72 Mev. It will be noted that the energy balance $0.72 + 6.89 = 7.61$ Mev is within ex-

perimental error of the value 7.56 Mev calculated from the mass values. The agreement of the absolute yields for these two lines with one another is an indication of the internal consistency of the measurements and an indirect check of the $\text{F}^{19}(p,\alpha\gamma)$ yield. The small amount of 1.43-Mev radiation was assumed to also cascade through the 0.72-Mev state, thus giving rise to a 5 percent correction (see Table I, and Fig. 10). The average value of $1.0_0 \pm 0.1$ cascades per 10^9 protons agrees well with the value reported by Fowler and Lauritsen.⁴ The simplest explanation for the 2.0–2.5 Mev radiation,

TABLE I. The absolute thick (Be metal) target yield of γ rays.^a

| Thick target 860 kev | | 993 kev resonance (7.48 Mev in B^{10}) $\Gamma = 88 \pm 3$ kev | | 1085 kev resonance (7.56 Mev in B^{10}) $\Gamma \approx 4$ kev | |
|-------------------------|----------------------|--|----------------------|--|----------------------|
| E_γ (Mev) | Yield $\gamma/10^9p$ | E_γ (Mev) | Yield $\gamma/10^9p$ | E_γ (Mev) | Yield $\gamma/10^9p$ |
| 0.41 | 0.05 ± 0.01 | 0.41 | $0.2_6 \pm 0.06$ | 0.41 | ≤ 0.008 |
| 0.72 | $1.0_6 \pm 0.2$ | 0.72 | 2.3 ± 0.4 | 0.72 | $1.0_6 \pm 0.2$ |
| 1.02 | $0.3_9 \pm 0.1$ | 1.02 | 0.6 ± 0.2 | 1.02 | ≤ 0.04 |
| 1.43 | 0.12 ± 0.03 | 1.43 | ≈ 0.3 | 1.43 | ≈ 0.05 |
| 1.78 | 0.07 ± 0.02 | | | | |
| 2.1 ₅ | ≤ 0.03 | | | 2.0–2.5 | $\approx 0.1–0.2$ |
| 5.2 | $0.3_2 \pm 0.1$ | | | | |
| 6.2 | ≈ 0.2 | | | 6.8 ₉ | $0.9_3 \pm 0.2$ |
| 7.1 | $1.5_4 \pm 0.4$ | 7.5 | 18.9 ± 5.0 | | |

^a The errors on the absolute yields are indicated; the relative errors are approximately one-half as large. The results given are in most cases the average of several runs.

TABLE II. Theoretical radiation widths.

| Level (Mev) | E1 | E2 | E3 | Γ_γ (ev) | | |
|----------------|-----|----------------------|----------------------|----------------------|----------------------|----------------------|
| | | | | M1 | M2 | M3 |
| ground | 185 | 0.045 | 7.9×10^{-6} | 8.8 | 2.2×10^{-3} | 3.7×10^{-7} |
| 0.72 | 130 | 0.026 | 3.9×10^{-6} | 6.5 | 1.3×10^{-3} | 1.8×10^{-7} |
| 1.74 | 83 | 0.013 | 1.2×10^{-6} | 3.9 | 6.0×10^{-4} | 5.7×10^{-8} |
| 2.15 | 67 | 8.5×10^{-3} | 7.5×10^{-7} | 3.2 | 4.3×10^{-4} | 3.5×10^{-8} |
| 3.58 | 26 | 1.8×10^{-3} | 8.6×10^{-8} | 1.2 | 9.0×10^{-5} | 3.9×10^{-9} |
| 5.11 | 5.5 | 1.4×10^{-4} | ... | 0.28 | 6.7×10^{-6} | ... |
| 5.17 | } | | | | | |
| ~6 | | | | | | |

in view of the absence of any 5.0–5.5 Mev γ radiation of comparable yield and the agreement of the 0.72- and 6.89-Mev γ -ray intensities,¹⁰ is that this radiation represents a transition to states at 5.0–5.5 Mev in B^{10} which then decay by α -particle emission to Li^6 .

A cascade beginning by a transition from the narrow proton resonance level to a state in B^{10} above 4.5 Mev most likely would be arrested by α -particle decay to Li^6 ; hence, any intermediate cascade population of the state at 1.74 Mev in B^{10} would proceed mainly through the states at 3.58 and 2.15 Mev, principally through the latter with an accompanying 0.41-Mev γ ray. The absence of any 0.41-Mev γ radiation indicates that the above mode of population of the 1.74-Mev level does not occur. Since no 1.02-Mev γ ray is observed (the 1.74-Mev state decays principally to the 0.72-Mev state), the remaining mode of population of the 1.74-state, that is, a direct transition from the proton capture state, does not occur either, which is consistent with the assignment of a 0^+ character to both of these two states.

The predominant radiative decay of the broad resonance is by the direct transition to the ground state (see Table I, and Fig. 10). In addition to the radiative level widths, the particle widths estimated from the experiments of Thomas *et al.*¹¹ are also indicated in Fig. 10.¹² Extensive use has been made of the $Be^9(d,n\gamma)$ work (see reference 1) in constructing the decay scheme.

Table II gives the radiative widths predicted from the formulas of Blatt and Weisskopf¹³ for various pos-

¹⁰ Note that if the 2.0–2.5 Mev radiation were between low-lying states in B^{10} , the known mode of decay of these states from the $Be^9(d,n\gamma)$ reaction would predict a substantial cascade through the state at 0.72 Mev.

¹¹ Thomas, Rubin, Fowler, and Lauritsen, *Phys. Rev.* **75**, 1612 (1949).

¹² It has been assumed for simplicity that resonant deuteron and α -particle emission is from the 993-keV state which is evident in the resonant γ -ray yield.

¹³ J. M. Blatt and V. F. Weisskopf, *Theoretical Nuclear Physics* (John Wiley and Sons, Inc., New York, 1952).

sible multipole transitions from the two prominent proton resonance levels to several of the states in B^{10} . The widths for the 993-keV resonance are somewhat lower, and the values for the 1085-keV resonance somewhat larger than the average values given in Table II.

The observed widths for the two $M1$ transitions indicated in Fig. 10, originating at the narrow proton resonance, compare favorably with the values predicted in Table II. The absence of other radiations is consistent with the spin and parity assignments given.

The three $E1$ transitions shown originating at the broad proton resonance are seen to be slower than predicted, particularly the transitions to the states at 0.72 and 2.15 Mev. It should be pointed out that these transitions are isotopic spin forbidden if the proton resonance level is taken as $T=0$. This last assignment is required by the observed deuteron and α -particle emission, assuming that only one resonance level is involved.¹⁴

The $M2$ transition to the state at 1.74 Mev is seen to be considerably faster than predicted, which may indicate a substantial feeding of this state by a mode not illustrated in Fig. 10 or may relate to the previous footnote.

The thick-target yield of γ radiations at $E_p=860$ keV (see Table I) shows large cascade probabilities, possibly indicating that the principal level involved has 1^+ character. The amount of 1.78-Mev γ radiation observed with a thick target at this energy, relative to the 1.02-Mev radiation, is not consistent with the former γ ray being the $M3$ transition from the 1.74-Mev state to the ground state, the intensity of the 1.78-Mev γ ray being much too large. A possible explanation is that the 1.78-Mev γ ray is a cascade transition between higher excited states in B^{10} . Intensity and energy considerations suggest that the 6.2- and 5.2-Mev γ rays are transitions from the proton capture state to the first and second excited states in B^{10} at 0.72 and 1.74 Mev, respectively.

We are indebted to Dr. A. Schardt for mounting the NaI crystals used in this experiment. We are particularly grateful to Dr. E. M. Hafner and Dr. J. Weneser for many helpful discussions.

¹⁴ The possibility of the existence of two separate levels cannot be ruled out, particularly since somewhat more yield of 0.72- and 1.02-Mev radiation is observed in the region $900 < E_p < 960$ keV than can be accounted for by an 88-keV wide resonance at 993 keV. The agreement of the yield of energetic γ radiation (see Fig. 7) with the single-level dispersion formula is not necessarily a contradiction to the two-level hypothesis if the relative probability of the direct ground state transition to cascade is markedly different for the two levels.